Modulation of Emission Characteristics by Donor Substitution in Multiple Resonant Thermally Activated Delayed Fluorescent Emitters

A Thesis

submitted to

Indian Institute of Science Education and Research Pune for the partial fulfilment of the MS Degree Programme

by

Sundaravalli N.

20212008

Indian Institute of Science Education and Research Pune

Dr. Homi Bhabha Road,

Pashan, Pune 411008, India

April, 2024

Supervisor: Prof. Partha Hazra

IISER Pune

Certificate

This is to certify that this dissertation entitled “Modulation of Emission Characteristics by Donor Substitution in Multiple Resonant Thermally Activated Delayed Fluorescent Emitters” towards the partial fulfilment of the M.S. degree programme at the Indian Institute of Science Education and Research, Pune, represents the work completed by Sundaravalli N. at Indian Institute of Science Education and Research (IISER), Pune under the guidance of Prof. Partha Hazra, Professor, Department of Chemistry, during the academic year 2023-2024.

Signature of the student

Signature of the supervisor

Committee:

Name of your Guide: Prof. Partha Hazra

Name of Your TAC: Prof. Angshuman Nag

Place: Pune,

Date: 27-03-2024

This thesis is dedicated to my mentor, **Abhijit Chatterjee**

Declaration

I hereby declare that the content embodied in the thesis titled “Modulation of Emission Characteristics by Donor Substitution in Multiple Resonant Thermally Activated Delayed Fluorescent Emitters” are the results of the project work done by me at the Department of Chemistry, Indian Institute of Science Education & Research (IISER) Pune, under the guidance of Prof. Partha Hazra, and this has not been submitted anywhere else for any other degree. Wherever other people contribute, all the efforts are taken to mention this clearly, with due reference to the research literature and acknowledgement of collaborative research and discussions.

Name: Sundaravalli N.

Date: 27-03-2024

Signature of the student

Acknowledgements

I am grateful to my thesis supervisor, Prof. Partha Hazra, for providing me with the opportunity to carry out research in his laboratory and supporting me in my progress and to my TAC member, Prof. Angshuman Nag, for his constant support. I am extremely beholden to my mentor, Mr Abhijit Chatterjee, who is also the joint lead of this project, providing valuable insights into the synthesis and contributing equally to the photophysical and computational parts. He taught me all the skills required and has been a constant motivation throughout. I am grateful to my lab members, Mr. Joy Chatterjee, Mr. Madhusudan Dutta, Ms. Anwesha Bera, Mr. Sowbhick Patra and others. They have motivated me in every step of my MS tenure, and it would have been difficult to pursue without their continuous encouragement. I especially would like to thank my lab member, Dr. Sandhya Nayak, who assisted me in revising my thesis. I am thankful to all the technical and non-technical staff of the department and institute as well. I am fortunate to have my parents - Amma and Appa, my sister Rajalakshmi and my friends at IISER, Rajdip and Pavithra, who have been mental support to me throughout my days at IISER.

Table of Contents

List of Figures

Abstract

Thermally Activated Delayed Fluorescence (TADF) is an emission phenomenon of paramount significance, owing to the fact that it renders access to the triplet excitons without the employment of heavy metals for enormous applications, especially in optoelectronics. However, owing to the substantial structural distortion in their excited state, imparted by the Intramolecular Charge Transfer (ICT) nature, the emission spectra of these compounds are typically broad, lowering the colour purity, which causes energy losses in optoelectronic devices. Addressing the aforementioned issue in this project, two molecules, comprising of quinolino[3,2,1-de]acridine-5,9-dione (QAO) as the core, are designed to exhibit charge transfer nature, wherein two kinds of donors, carbazole and diphenylamine, are incorporated respectively. The core moiety QAO is known to manifest Short Range Charge Transfer (SRCT) on account of the electronic density distribution brought about by the opposite mesomeric effects in their components and the SRCT prompts narrowing of the emission spectra. Preliminary results reveal that carbazole, being a weaker donor, imparts a reduced ICT character and, therefore, partially retains the SRCT nature, unlike diphenylamine, which induces an absolute ICT nature. Therefore, by establishing a trend in these compounds, investigation of the structure-property correspondence at the molecular level becomes feasible, facilitating tuning of the emission spectra for cutting-edge applications.

1. Introduction:

Organic Light Emitting Diodes (OLEDs) have received remarkable attention owing to their lightweight design, higher contrast ratio, broader viewing angles, and ease of fabrication on flexible substrates.[1–3] In OLED technology, charge carriers are introduced through electrodes, traverse various layers, and recombine at the organic emitting layer to form excitons. These excitons undergo radiative decay, emitting light through electroluminescence.[4] Spin statistics dictate that the electrons and holes recombine to yield singlet and triplet excitons in a ratio of 1:3.[5,6] In pure organic scaffolds, the triplets are usually dark owing to the minimal Spin-Orbit Coupling (SOC) between the triplet and the singlet.[7] Thus, harvesting triplet excitons in pure organic molecules is of utmost importance for improving the efficiency and cost-effectiveness of OLEDs. Various photophysical phenomena have been explored in an attempt to harvest the otherwise dark triplet excitons, including Room Temperature Phosphorescence (RTP),[8,9] Triplet-Triplet Annihilation (TTA),[10] and TADF.[11]

Among these, TADF (Figure 1a) offers access to harvesting the whole of triplet excitons without the use of expensive metals, with an Internal Quantum Efficiency (IQE) of 100%. To achieve efficient TADF, the singlet and triplet excited state of the lowest energy should be close enough (ΔE_{ST} < 0.3 eV) [11] for the upconversion of triplet excitons to singlets to be supported by the thermal energy of room temperature. This small ΔE_{ST} is brought about by separating the Highest Occupied Molecular Orbital (HOMO) and Lowest Unoccupied Molecular Orbital (LUMO),[12,13] which in turn reduces the exchange integral value between the Singly Occupied Molecular Orbitals (SOMO) in the excited state.[14] This is accomplished through a widely accepted donor-acceptor (D-A) molecular design with Charge Transfer (CT) emissive states[15] (Figure 1b).

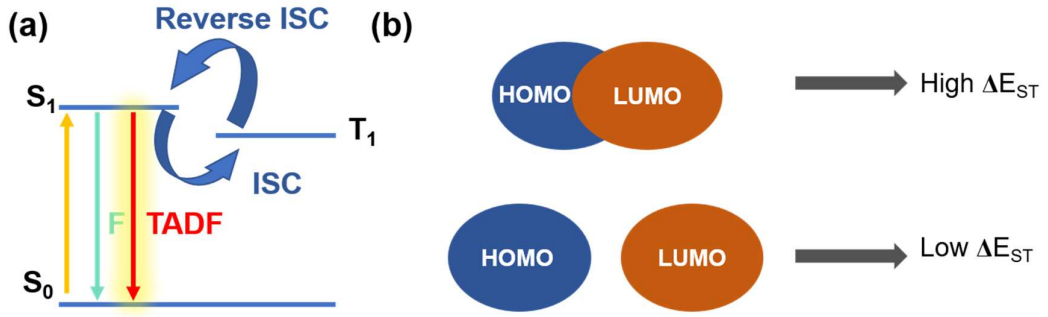

Figure. 1 a) TADF **b)** Schematic representation for controlling the ΔE_{ST}.

However, the low ΔE_{ST}, as a result of the imparted ICT character in these conventional D-A type molecules, is accompanied with small oscillator strength corresponding to the S_1-S_0 transition as both of them are essentially dependent on the HOMO-LUMO overlap.[16] This is crucial since the photoluminescence quantum yield (PLQY) is a function of the oscillator strength[17] and a low value of oscillator strength brings down the PLQY, which will ultimately have an impact on the External Quantum Efficiency (EQE) of the device.[18,19]

In addition, the ICT nature of conventional TADF molecules causes broadening of the emission spectra with a Full Width at Half Maxima (FWHM) of 70-100 nm (Figure 2a).[11,14] Thus, the broad emission of these D-A based TADF molecules renders them colour impure and often requires the usage of optical microcavities or colour filters[20] to improve the colour purity of the electroluminescence (EL), resulting in enormous energy losses in the industrial scale. The RGB emission spectra of the display in Samsung galaxy S5[14] is displayed in Figure 2b, to form a notion of the spectral characteristic requirements for optoelectronic display devices such as OLEDs.

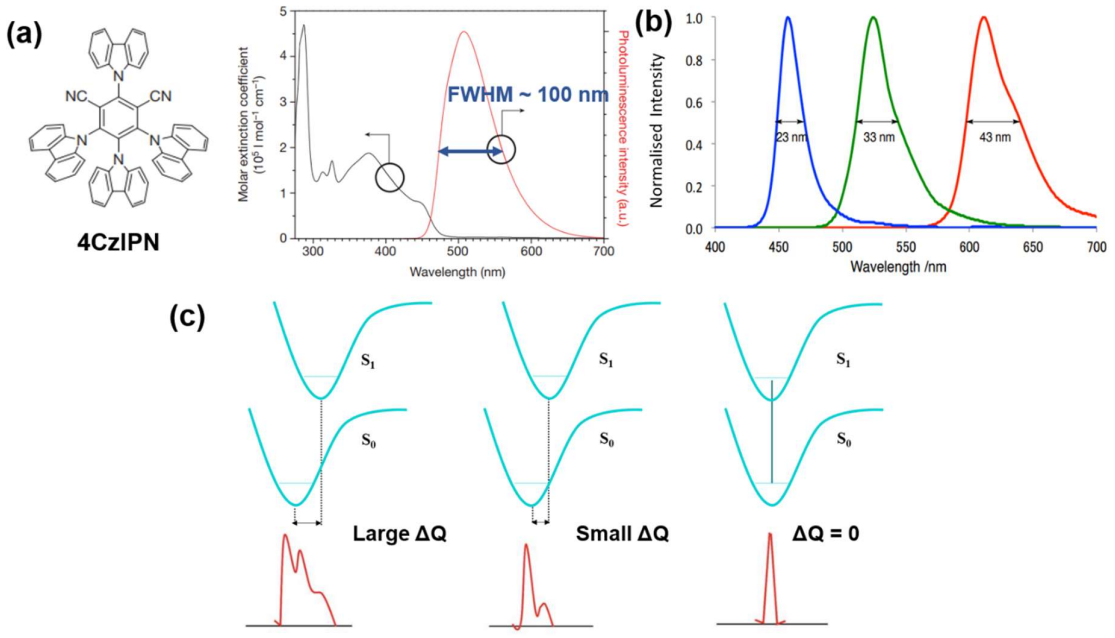

Figure. 2 a) Conventional TADF molecule 4CzIPN and its emission profile[11] **b)** RGB emission spectra of the OLED display in Samsung Galaxy S5 along with its FWHM[14] **c)** Correlation between excited state structural distortion ΔQ and emission bandwidth

The interdependence of the emission broadening and the excited state reorganisation can be visualised by considering the Huang Rhys (HR) factor, S[21,22]

which measures the distortion in structure of the excited state (ΔQ) with respect to the ground state. Large value of ΔQ is accompanied with coupling of multiple vibronic progressions resulting in broad emission bandwidth and vice versa.[21] (Figure. 2c) In CT transitions,[15] the redistribution of the electron density during electronic transitions is huge,[23,24] triggering large vibronic coupling between the S_0 and S_1 excited states,[25,26] and greater structural relaxation in the singlet S_1. This can be considered in correlation with the large Stokes shift observed in these CT molecules.[14,27]

Therefore, in order to bring about low ΔE_{ST} with high PLQY and narrow FWHM, a new strategy for TADF with boron and nitrogen framework was proposed based on Multiple Resonance effect by Hatakeyama and co-workers in 2016.[14,27,28] Since nitrogen shows an opposite resonance effect of boron atoms in an aromatic ring, careful molecular engineering makes it possible to concentrate the HOMO and LUMO on electron-rich and electron-deficient parts of the aromatic ring, without having to entirely isolate the molecular orbitals (Figure 3).[14,27]

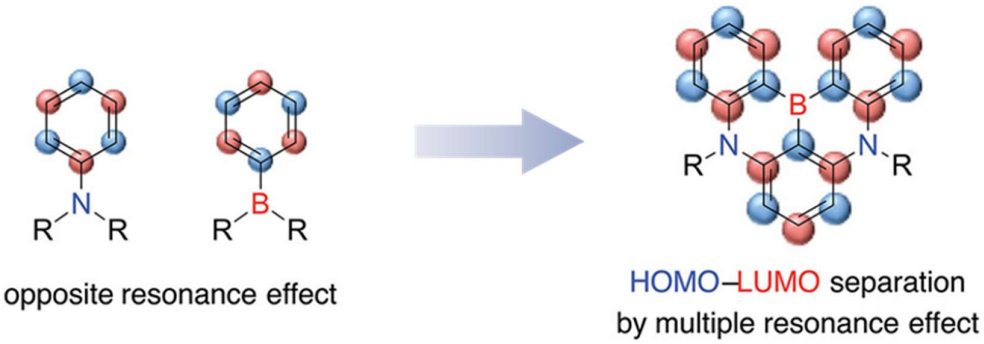

Figure 3. Pictorial illustration of Multiple resonance effect in B-N organic framework[14]

Hence, a sufficient separation of HOMO-LUMO (Short Range Charge Transfer or SRCT) is effectuated for ΔE_{ST} to be low but not large enough to result in significant structural distortion in the excited state. The rigid framework of Multiple Resonant Thermally Activated Delayed Fluorescent (MR-TADF) molecules ensures good oscillator strength of excited state in this molecular design facilitating appreciable PLQY, while maintaining less excited state distortion, ΔQ.

1.1. Molecular Design and Motivation:

In this project, a quinolino[3,2,1-de]acridine-5,9-dione (QAO) core is chosen where the design of the core has its basis on the complementary nature of the resonance effect due to the carbonyl and amine groups (Figure 4a).[29–32]

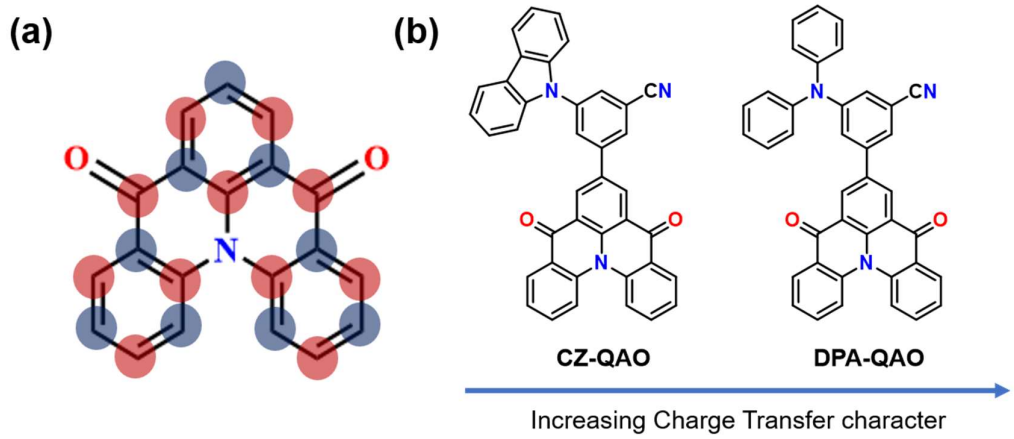

Figure 4. a) Schematic representation of localisation of HOMO-LUMO in QAO core **b)** Structures of the designed molecules - CZQAO and DPAQAO

The structure of the designed molecules by donor substitution onto QAO core is shown in Figure 4b. The incorporation of donor moieties brings about more Long Range Charge Transfer (LRCT) in comparison with the core, as QAO tend to behave as an acceptor in the presence of a donor.[29] Carbazole, being a weaker donor, is expected to retain the SRCT of the core, whereas diphenylamine would achieve complete ICT, thereby establishing a trend in the properties affected by the charge transfer nature. By investigating the effect of these substituents on the Reverse Inter System Crossing (RISC) rates, excited state reorganisation and the radiative and the non-radiative decay rates, we will be able to gain insights into the structure-property correspondence of the Multiple Resonant cores and the modulation of their emission characteristics becomes feasible for futuristic technological applications.

2. Materials and Instrumentation:

For the purpose of synthesis, chemicals such as diphenyl amine, carbazole, sodium hydride, copper (I) iodide, potassium carbonate, o-dichlorobenzene, sodium hydroxide, oxalyl chloride, Tin (IV) chloride, $Pd(PPh_3)_4$, Potassium acetate and bis(pinacalato)diboron are purchased from Sigma Aldrich. Other reagents, such as 3-bromo-5-fluorobenzonitrile and dimethyl 5-bromo-2-iodoisophthalate, are purchased from Tokyo Chemical Industry (TCI) and Combi Block, respectively. All of these are used directly without any attempt to purify them further. Spectroscopy grade solvents from Spectrochem. Pvt. Ltd. are used for solution based photophysical studies.

Quantum chemical results are calculated by making use of the Gaussian 09 package using a cluster facility, Param Brahma, made available by IISER Pune. Initially, the optimisation of ground state geometry is calculated in the gas phase and it is confirmed to be the global minimum by frequency analysis[33,34]. These calculations are done at the B3LYP/6-31G (d, p) level. Moreover, Time Dependent Density Functional Theory (TD-DFT) is performed to visualise the distribution of HOMOs and LUMOs in space and also to obtain the energies of singlet and triplet excited states employing Time Dependent-Self Consistent Field (TD-SCF) method.[35]

High-Resolution Mass Spectrometry (HRMS) was performed in Water's SYNAPT G2 mass spectrometer using ESI-TOF method. ^{1}H NMR (at 400 MHz) and ^{13}C NMR (at 100 MHz) characterisations of all the synthesised compounds were measured using JEOL ECS-400 and Bruker AscendTM 400 spectrometer with $CDCl_3$ acting as the solvent and tetramethylsilane (Me_4Si) as the NMR standard. Steady-state absorption spectra were collected in UV-2600 spectrophotometer. Emission spectra in all the states were carried out using a FluoroMax-4 Series HORIBA spectrofluorometer. The emission decays were carried out with the help of the DAS6 Fluorescence Decay Analysis Software from HORIBA with a diode laser source or a spectra LED source. The data was fitted by examining χ^2-values and visually inspecting residuals where the fit with χ^2 = (1-1.2) value is taken as the best fit.

3. Results and Discussion:

3.1. Synthesis and Characterisation:

Both the compounds CZ-QAO and DPA-QAO are designed to be synthesised by Suzuki Coupling of the pre-cursor QAO-Br with their respective boronic esters[36]. The boronic ester formation was carried out *in situ* via Miyuara Borylation[37] catalysed by a palladium complex. The synthetic route and the intermediate steps of both the two compounds is outlined in Figure. 5 (a, b, c).

Figure. 5 a) General synthesis outline:

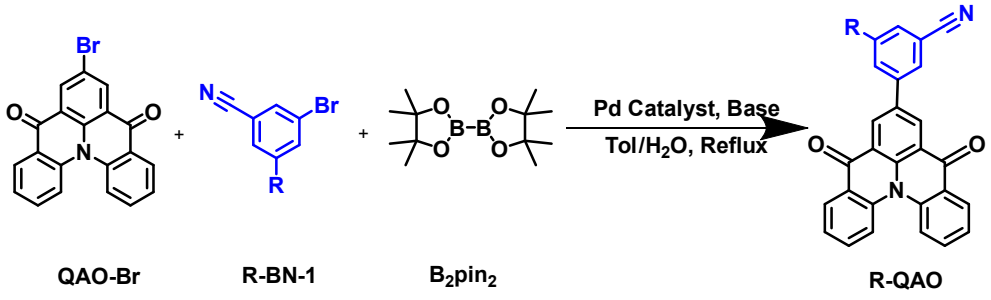

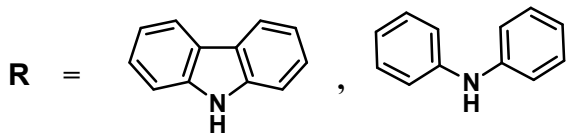

b) Synthesis of QAO-Br:

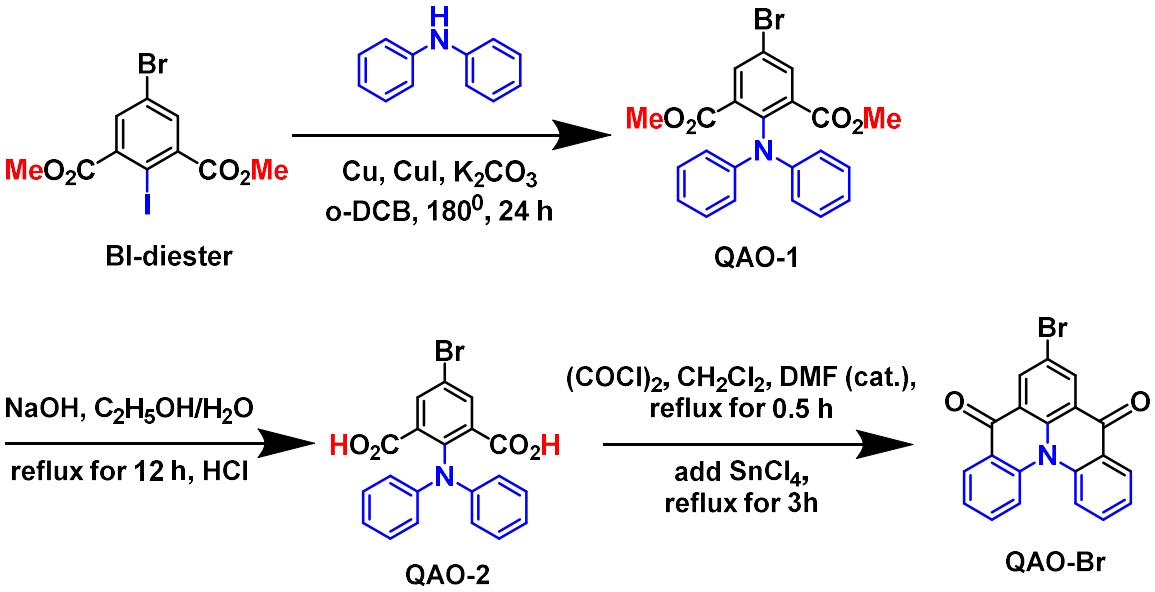

c) Synthesis of R-BN-1:

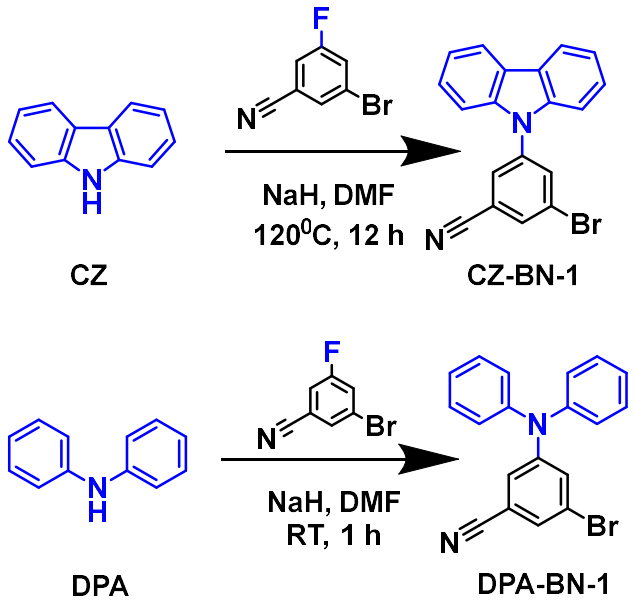

3.1.1. <u>Synthesis of QAO-1 (Dimethyl 5-bromo-2-(diphenylamino)isophthalate):</u>

A mixture of dimethyl 5-bromo-2-iodoisophthalate (BI-diester, 1 g, 2.51 mmol), diphenylamine (0.51 g, 3.01 mmol), activated copper powder (0.063 g, 1.00 mmol),

copper(I)iodide (0.024 g, 125.32 µmol), K_2CO_3 (0.45 g, 3.26 mmol) and 10 mL 1,2-dichlorobenzene (o-DCB) was refluxed with stirring for 24 hours and maintained under a continuous flow of nitrogen. After the reaction mixture was cooled to room temperature (RT), 25 mL dichloromethane (DCM) was poured and stirred for 10 minutes. Then, the mixture was filtered and the concentrated filtrate was purified through silica gel column chromatography using EtoAc/Pet. ether solvent mixture as the mobile phase. (Yield: 990 mg, 90%).

HRMS (ESI TOF): m/z calculated. For $C_{22}H_{18}BrNO_4$ $[M]^+$ 439.0419, found 439.0419. (Appendix)

3.1.2. Synthesis of QAO-2 (5-bromo-2-(diphenylamino)isophthalic acid):

Dimethyl 5-bromo-2-(diphenylamino)isophthalate (0.9 g, 2.04 mmol) and sodium hydroxide (0.41 g, 10.22 mmol) were added to a solution of ethanol/water (1/1, 30 mL). The mixture was allowed to reflux with stirring for 12 hours. Once the mixture attains RT, precipitation with conc. HCl yields the yellow solid, which was filtered with a glass filter funnel, washed with deionized water and air dried. The yellowish brown solid product was used for further reactions without any purification.

HRMS (ESI TOF): m/z calculated for $C_{20}H_{14}BrNO_4$ $[M-H]^+$ 410.0028, found 410.0020. (Appendix)

3.1.3. Synthesis of QAO-Br (7-bromoquinolino[3,2,1-de]acridine-5,9-dione)[36,38]:

Catalytic amount of dimethylformamide (DMF) was added to 5-bromo-2-(diphenylamino)isophthalic acid (QAO-2) (0.8 g, 1.94 mmol) in 30 mL of dry DCM. Oxalyl chloride (0.36 mL, 4.27 mmol) was dropped into the mixture and left to reflux for half an hour. Then, Tin (IV) chloride (0.5 mL, 4.27 mmol) was dropwised and the reflux condition was maintained for 3 more hours. Once the reactant was consumed, the mixture was neutralised with 1 M NaOH under constant stirring and extracted with DCM. The organic layer was passed over anhydrous Na_2SO_4 and purified by neutral alumina column chromatography to give an orange-yellow solid product. (Yield: 700 mg, 77%)

^{1}H NMR (400 MHz, $CDCl_3$) δ in ppm: 8.81 (s, 2H), 8.48 (dd, *J* = 7.9, 1.5 Hz, 2H), 8.13 (d, *J* = 8.6 Hz, 2H), 7.82 – 7.62 (m, 2H), 7.51 (t, *J* = 7.5 Hz, 2H).

HRMS (ESI TOF): m/z calculated or $C_{20}H_{10}BrNO_2$ $(M+H)^+$ 375.9973, found 375.9962. (Appendix)

3.1.4. Synthesis of CZ-BN-1[39] (3-bromo-5-(9H-carbazol-9-yl)benzonitrile):

9H-carbazole (2.3 g, 13.76 mmol) in dry DMF was added into a dispersion of NaH (60%, 330.09mg, 13.76 mmol) in dry DMF kept in a bath of ice under stirring. After 1 hour, 3-bromo-5-fluorobenzonitrile (3 g, 14.99 mmol) in anhydrous DMF (50 mL) was added to the mixture under a continuous flow of nitrogen. The mixture was allowed to be proceed at 120^0C for 12 hours. Once the starting material gets consumed, the organic part was extracted with DCM, and dried using anhydrous Na_2SO_4 to be concentrated in vacuo. The reaction product was purified by SiO_2 column chromatography using $CHCl_3$/Pet. ether as the eluent. (Yield = 3.5 g, 89%)

^{1}H NMR (400 MHz, $CDCl_3$) δ in ppm: 8.14 (d, J = 7.7 Hz, 2H), 8.02 (t, J = 1.8 Hz, 1H), 7.86 (dt, J = 4.5, 1.4 Hz, 2H), 7.51 – 7.42 (m, 2H), 7.43 – 7.30 (m, 4H).

^{13}C NMR (101 MHz, $CDCl_3$) δ in ppm: 139.85 (d, J = 22.5 Hz), 134.26 (s), 132.93 (s), 128.62 (s), 126.38 (s), 123.86 (d, J = 15.0 Hz), 121.07 (s), 120.51 (s), 116.42 (s), 115.39 (s), 109.02 (s). (Appendix)

3.1.5. Synthesis of DPA-BN-1 (3-bromo-5-(diphenylamino)benzonitrile):

A solution of diphenylamine (375 mg, 2.22 mmol) in anhydrous DMF was added into a dispersion of NaH (60%, 265.89 mg, 11.08 mmol) in anhydrous DMF kept in a bath of ice under constant stirring. After approximately 20 minutes, when the solution started turning green, 3-bromo-5 fluorobenzonitrile (483.10 mg, 2.42 mmol) in anhydrous DMF (5 mL) was added to the reaction mixture under a continuous flow of nitrogen. The mixture was allowed to proceed at RT for 1 hour. The organic part was extracted with DCM, dried with anhydrous Na_2SO_4 and concentrated. The product was purified by silica column chromatography. A white product was obtained which was characterized by ^{1}H, ^{13}C NMR and HRMS. (Yield = 0.5 g, 64%).

^{1}H NMR (400 MHz, $CDCl_3$) δ in ppm: 7.38 – 7.29 (m, 5H), 7.24 (t, J = 1.5 Hz, 1H), 7.20 – 7.14 (m, 2H), 7.14 – 7.08 (m, 5H).

^{13}C NMR (101 MHz, $CDCl_3$) δ in ppm:150.36 (s), 146.24 (s), 130.44 (s), 127.74 (s), 126.59 (s), 126.14 (s), 125.67 (s), 123.72 (s), 122.76 (s), 117.98 (s), 114.80 (s).

HRMS (ESI TOF): m/z calculated for $C_{19}H_{13}BrN_2$ $[M+H]^+$ 349.0340, found 349.0345. (Appendix)

3.1.6. Synthesis of CZ-QAO (3-(9H-carbazol-9-yl)-5-(5,9-dioxo-5,9dihydroquinolino [3,2,1-de]acridin-7-yl)benzonitrile)

A mixture of QAO-Br (0.15 g, 0.398 mmol) and CZ-BN-1 (0.14 g, 0.398 mmol), bis(pinacalato)diboron (B_2pin_2) (0.12 g, 0.478 mmol), KOAc (273.5 mg, 2.79 mmol), Toluene (7 mL) and deionised water (3 mL), with $Pd(PPh_3)_4$ (0.14 g, 0.119 mmol) as the catalytic reagent was heated with reflux at 110^0C for 24 hours. Once the reactant was consumed, the mixture attains RT and extracted with DCM. The resulting mixture was purified by neutral alumina column chromatography to give a yellow solid product.

^{1}H NMR (400 MHz, $CDCl_3$) δ in ppm: 8.99 (s, 2H), 8.52 (dd, *J* = 7.9, 1.6 Hz, 2H), 8.26 (s, 1H), 8.18 (d, *J* = 7.5 Hz, 5H), 7.96 – 7.94 (m, 1H), 7.78 – 7.71 (m, 2H), 7.54 (t, *J* = 7.5 Hz, 2H), 7.50 – 7.46 (m, 4H), 7.36 (ddd, *J* = 8.0, 5.7, 2.5 Hz, 2H).

HRMS (ESI TOF): m/z calculated for $C_{39}H_{21}N_3O_2$ $(M+H)^+$ 564. 1712, found 564.1709. (Appendix)

3.1.7. Synthesis of DPA-QAO (3-(5,9-dioxo-5,9-dihydroquinolino[3,2,1-de]acridin-7-yl)-5-(diphenylamino)benzonitrile)

A mixture of QAO-Br (0.05 g, 0.132 mmol), DPA-BN-1 (0.046 g, 0.132 mmol), B_2pin_2 (0.04 g, 0.160 mmol), KOAc (91 mg, 0.93 mmol), Toluene (3 mL) and deionised water (1 mL), with $Pd(PPh_3)_4$ (0.05 g, 0.04 mmol) as the catalytic reagent was heated with reflux at 110^0C for 24 hours. Once the reactant was consumed, the mixture was allowed to attain RT and need to be purified by neutral alumina column chromatography to give the product.

HRMS (ESI TOF): m/z calculated for $C_{39}H_{23}N_3O_2$ $(M+H)^+$ 566. 1869, found 566.1860. (Appendix)

3.1. Theoretical studies:

To verify the viability of the molecular design, DFT calculations are performed. The geometry in the ground state for CZQAO and DPAQAO are optimised at B3LYP/ 6-31G (d, p) level, utilising the Gaussian 09 package. The HOMO and the LUMO are

visualised along with the ground state geometry in Figure 6a. The HOMO-LUMO gap is 3.64 eV and 1.79 eV in CZQAO and DPAQAO respectively.

In CZQAO, the distribution of electron densities in the MOs is not entirely isolated but rather localised on atoms in accordance with the multiple resonance effect incorporated into the molecular design. The increment in the donor strength from carbazole to diphenylamine is clearly evident in the HOMO-LUMO profile, with the LUMO remaining almost constant in both the compounds, while the HOMO gradually shifting towards the donor moiety. In contrast to the partial overlap of HOMO-LUMO in CZQAO, DPAQAO displays distinct separation between these orbitals, with the HOMO spread over the diphenylamine scaffold and the LUMO concentrated on the QAO core. Consequently, DPAQAO is anticipated to exhibit pronounced ICT characteristics in its optical properties. Consequently, DPAQAO is anticipated to exhibit pronounced ICT characteristics in its optical properties. The Franck-Condon excited state energies are calculated by employing the TD-SCF method (Figure 6c).

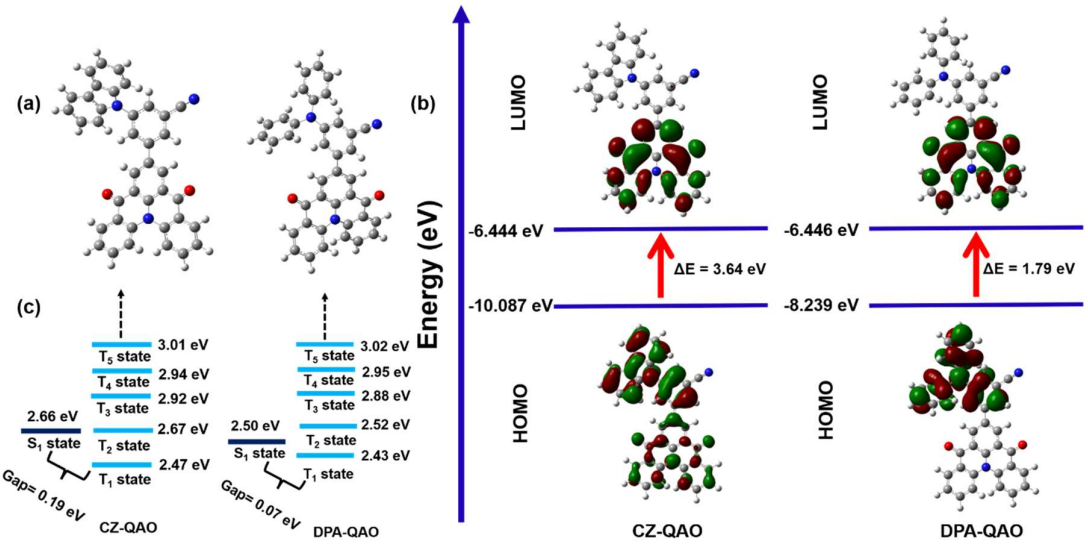

Figure. 6 DFT analysis of CZQAO and DPAQAO at B3LYP/6-31G (d.p) level **a)** Optimised ground state geometries **b)** Visualisation of HOMO and LUMO along with their energies **c)** Franck-Condon energies of excited states calculated by TD-DFT.

The ΔE_{ST} is 0.19 eV in CZQAO, which is reduced to 0.07 eV in DPAQAO, corresponding to the increase in the ICT nature. Considering the low ΔE_{ST} (< 0.3 eV) of both compounds, we expect that these molecules exhibit delayed fluorescence processes.

3.2. Photophysical Properties of CZQAO:

Absorption spectra of CZQAO in the solution state (Figure. 7a) exhibit two absorption bands. The bands of higher energy (300-400 nm) are assigned to the π-π* transitions of the QAO core and the donor carbazole moiety.[24] The lower energy band centred at 443 nm is attributed to the SRCT transitions, distinctive of MR-TADF molecules,[29–31] arising from the QAO core. The molecule has a sky-blue emission in toluene, peaked at 461 nm, and has a small FWHM of 29 nm (Figure. 7b), which suggests the effective molecular design of employing the Multiple Resonance effect. This interpretation is consistent with the small Stokes shift (17 nm) observed, indicating minimal reorganisation in the excited state as a result of the rigid molecular framework.

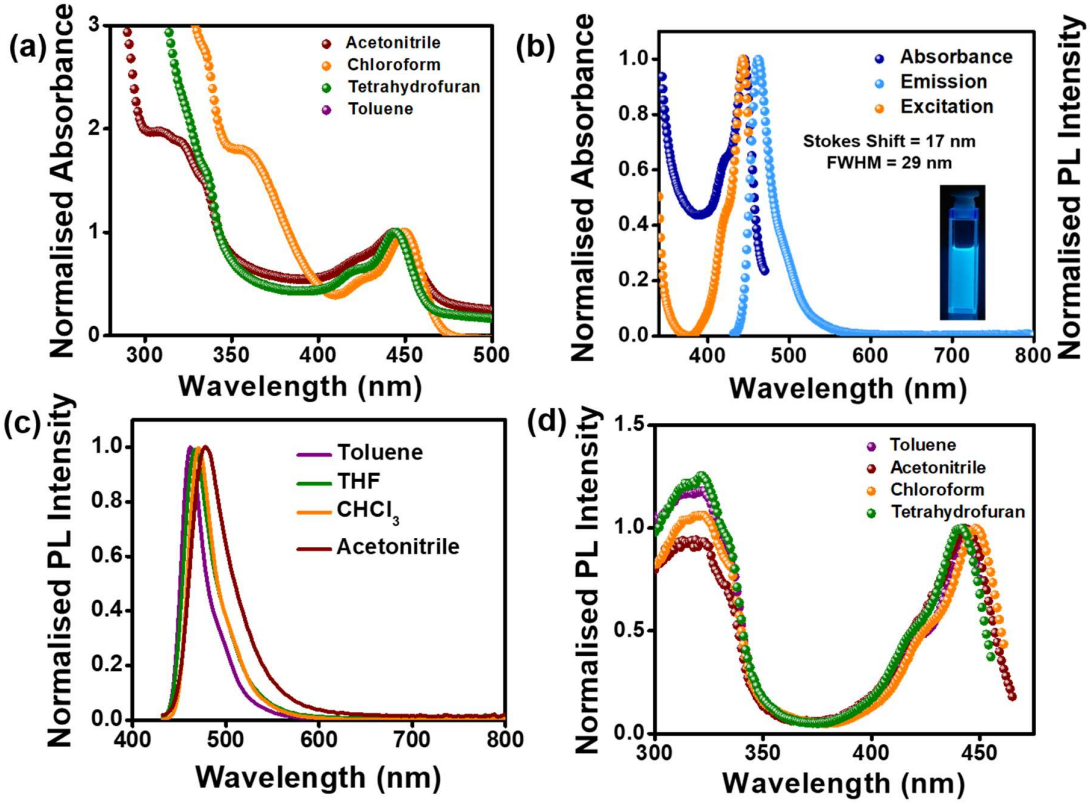

Figure. 7 a) Absorption spectra of CZQAO in various solvents with a concentration of 10 μM **b)** Absorption, Emission and Excitation spectra of CZQAO in 10 μM toluene solution **c)** Emission spectra of CZQAO in solvents of increasing polarity with a concentration of 10 μM (λ_{exc} = 410 nm) **d)** PL excitation spectra of CZQAO in various solvents

The steady state emission spectra of CZQAO in increasing polarity of solvents (Figure. 7c) depict a small degree of positive solvatochromism (17 nm shift from

Toluene to Acetonitrile), in contrast to the solvatochromism exhibited by conventional charge transfer molecules (typically 50-100 nm),[40,41] indicative of the SRCT nature. This is in correlation with the effect of increasing polarity on the FWHM of the emission spectra (29 nm for toluene, 37 nm for THF and $CHCl_3$, 50 nm for Acetonitrile). The PL excitation spectra (Figure. 7d) in different solvents match well with the absorption spectra in accordance with the Kasha's rule.[42]

Photophysical measurements were performed in degassed and aerated toluene in order to confirm TADF (Figure 8a). The emission spectrum in degassed toluene exhibits an increased PL intensity in comparison with its aerated form.

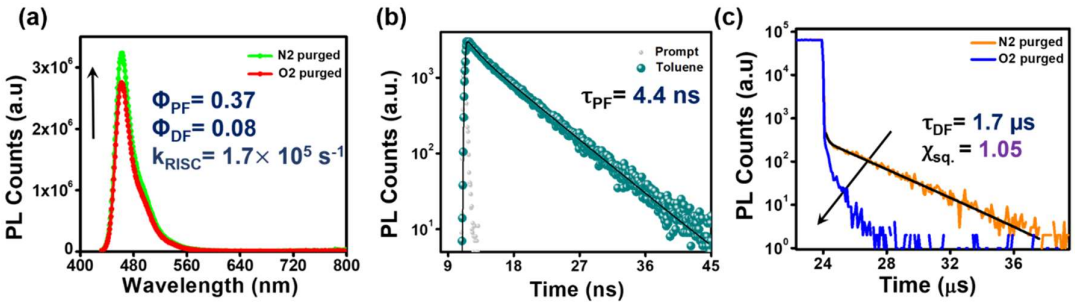

Figure. 8 a) Photoluminescence spectra of CZQAO in N_2 purged and O_2 purged conditions. λ_{exc} = 375 nm) **b)** Time-resolved fluorescence decay profile of CZQAO in 10 µM degassed toluene solution at RT (λ_{exc} = 375 nm) **c)** Delayed fluorescence lifetime of CZQAO in N_2 purged and O_2 purged conditions (λ_{exc} = 357 nm). Both lifetime decays are measured by collecting emission at 461 nm.

The investigation of the time-resolved PL (TRPL) decay has been carried out in Toluene at ambient temperature, which shows prompt (ns) and delayed (µs) components. The prompt component decay profile was found to be bi-exponential in nature, with an average lifetime of 4.4 ns (Figure 8b). The delayed fluorescence lifetime, collected in degassed toluene (N_2 purged) at 461 nm, is bi-exponential with an average value of 1.7 µs. This longer lifetime component was found to be entirely diminished in the aerated condition (O_2 purged), which occurs due to the energy transfer from the triplet of CZQAO to oxygen (Figure 8c). The emission profile and lifetime data together confirm the involvement of triplets in the delayed fluorescence process.

Since RISC is brought about by thermal activation at room temperature and is greatly influenced by the singlet-triplet activation barrier or ΔE_{ST} value, the steady state

PL (photoluminescence) spectrum is measured at 77K (Figure 9a). The spectrum manifests two emission peaks, one at 461 nm, associated with the steady-state emission at room temperature, corresponding to singlet emission. The other peak is red shifted centred at 505 nm, attributed to the phosphorescence emission (Figure 9b). The experimental ΔE_{ST} is calculated by the difference in energy of the two emission peaks at 77K and is found to be 0.23 eV, which is comparable to the computationally predicted ΔE_{ST} of 0.19 eV.

The absolute quantum yield measurement of CZQAO was found to be 0.45 in degassed toluene, where the fractional contribution of prompt and delayed fluorescence was measured from the toluene degassing experiment to be 0.37 and 0.08 respectively. The calculated RISC rate constant was found to be as high as 1.7 x 10^5 s^{-1} (Appendix), ensuring a strong RISC from triplet to singlet.

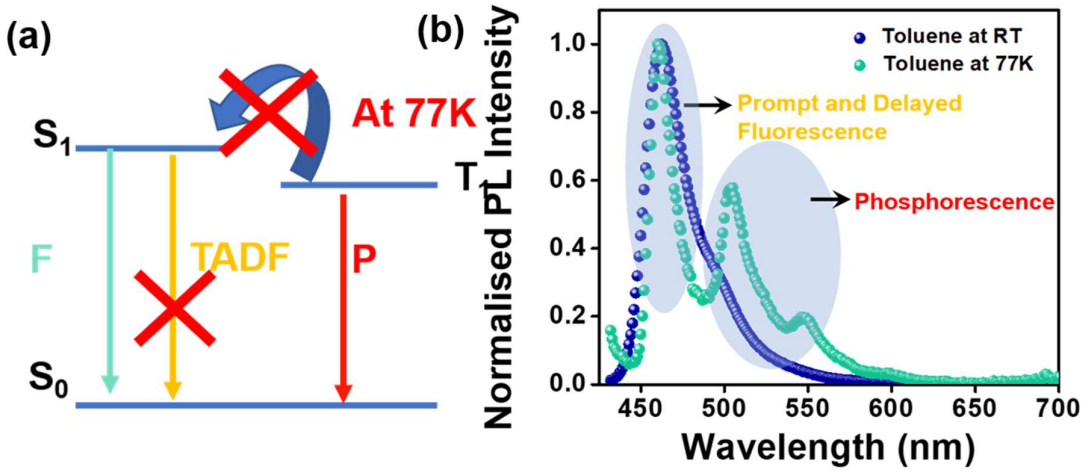

Figure. 9 a) Schematic diagram representing the fate of the excited state at 77K. **b)** Steady state photoluminescence spectra at RT and 77K (λ_{exc} = 410 nm)

The photophysical properties of CZQAO film in a Polymethylmethacrylate (PMMA) host matrix were studied to test its viability in OLED design at a doping concentration of one weight percent. Doping retains the monomeric property of molecules in the film by reducing the concentration quenching effect and emission broadening that occurs due to aggregation of molecules. PMMA is chosen as the host material owing to its triplet energy (~3.1 eV) which is high enough to prevent triplet energy transfer from the emitter. The photoluminescence spectrum at RT reveals a sharp peak at 464 nm with a slightly broadened FWHM of 38 nm compared to toluene

(Figure. 10a), presumably as a result of electronic interactions between the host and the emitter. Nevertheless, the emission colour purity is maintained and is verified by plotting the CIE (*Commission Internationale de l'éclairage*) chromaticity diagram (Figure. 10a inset). The CIE coordinates are (0.14, 0.15), comparable to the standard coordinates for blue colour set by the National Television Standards Committee (NTSC) (0.14, 0.08).

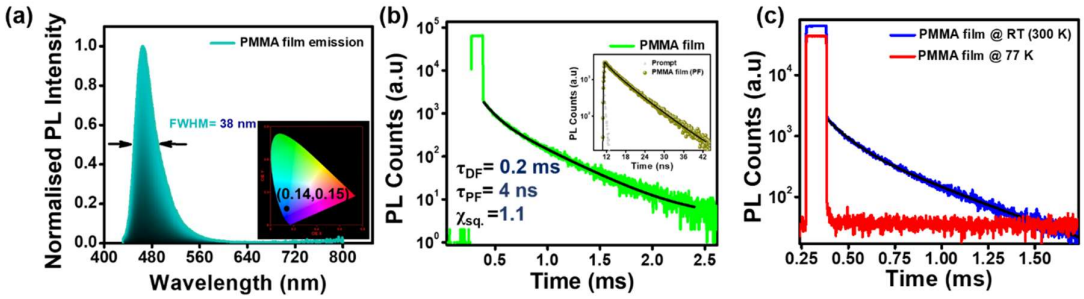

Figure. 10 a) Photoluminescence spectrum of 1 wt% CZQAO doped PMMA film at RT. Inset: CIE chromaticity diagram of the doped PMMA film. **b)** Time-resolved fluorescence decay profile of doped PMMA film at RT (λ_{em} = 464 nm) **c)** Comparison of delayed lifetimes collected at 464 nm of the doped PMMA film at RT and 77 K. All measurements are completed with λ_{exc} = 375 nm.

The time-resolved photoluminescence decay profile of the doped film at room temperature shows prompt and delayed lifetimes averaged to be 4 ns and 200 µs respectively (Figure 10b). Notably, the delayed lifetime component in the sub-millisecond range almost vanishes entirely at liquid nitrogen temperature, with the appearance of a long tail assigned to phosphorescence (Figure 10c). This directly proves the 'thermally activated' TADF process. The film shows ultralong phosphorescence with an afterglow, occurring due to the restriction of RISC and activation of triplet states at cryogenic temperature (Figure 9a).

Interestingly, CZQAO neat film's emission profile exhibited two peaks at around 495 nm and 575 nm. The low energy emission band is broader, with a FWHM of 115 nm. To investigate the emergence of this peak, aggregation-based studies were carried out by gradually increasing the water content of the CZQAO solution in THF. Figure 11a shows an initial solvatochromic shift that is observed when the water concentration is progressively increased from 0% to 50%, resulting in a shift from 466 nm to 490 nm. As the water concentration approaches 95%, a low-energy broad

emission band emerges, centred at 570 nm, along with a relatively narrower peak at around 495 nm.

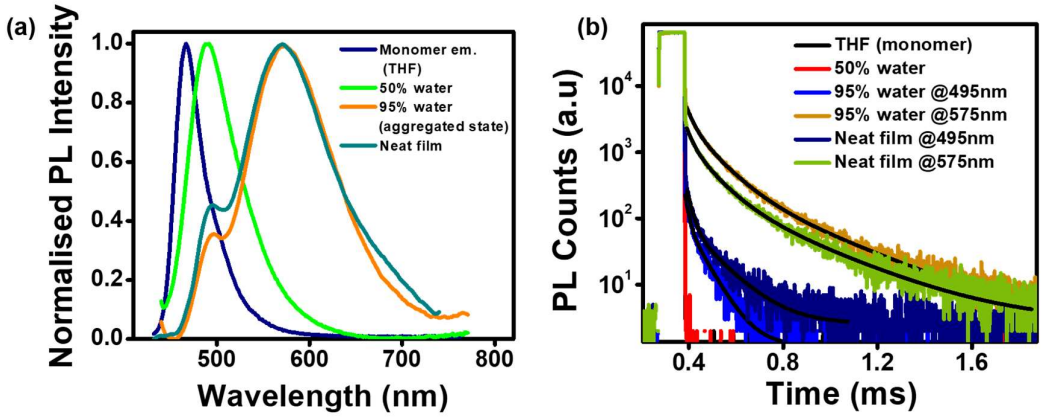

Figure. 11 a) Aggregation based photoluminescence studies of CZQAO **b)** Photoluminescence decay profiles of CZQAO in monomer, aggregated and neat film states. (λ_{exc} = 375 nm)

The delayed lifetime profiles of the neat film and the solution with 95% water content are collected at 495 nm and 575 nm (Figure 11b). The delayed fluorescence lifetime measured at 575 nm for both states is similar (89 µs and 85 µs for 95% water and neat film, respectively), suggesting the formation of the same excited emissive states upon aggregation.

The bathochromic shift in the emission and the broadening of the peak surely indicates higher structural reorganisation of the aggregated emissive species and still need further experimentation to code out its origin and nature.

4. Conclusions:

We have designed two molecules CZQAO and DPAQAO, by substituting donor moieties onto the Multiple Resonant QAO core, where the synthesis and characterisation of CZQAO and DPAQAO has been successfully completed. DFT analysis depict SRCT and LRCT nature in CZQAO and DPAQAO respectively with low ΔE_{ST} values and thus are expected to exhibit TADF nature. The photophysical studies of CZQAO are carried out in solution state and doped PMMA film and the molecule is proven to show narrow band emission with appreciable PLQY. The small Stokes shift and narrow FWHM indicates limited structural distortion in the excited state, and the SRCT nature of the molecule is analysed with solvatochromic studies, in compliance with the computational results. TADF is confirmed to be shown in this molecule,

exemplified by the toluene degassing and temperature dependent PL measurements in both solution and film states. Colour purity in emission is demonstrated by plotting the CIE chromaticity diagram and CZQAO has CIE values in par with the NTSC standards. The broadening of emission in the neat film is investigated with aggregation-based studies and the higher structural reorganisation in neat film needs to be further explored.

4.1. Future Plans:

- Delayed emission spectra of CZQAO at room temperature and low temperature have to be measured in Toluene solution and doped PMMA film in order to get further insights into the TADF process.
- After purification of DPAQAO, photophysical studies of DPAQAO need to be carried out so that the effect of the ICT nature on the excited state reorganisation of this molecule can be investigated in comparison with CZQAO.
- We will perform further computational investigation of CZQAO and DPAQAO in the excited state and correlate them with their optical properties.
- Electroluminescence properties of these molecules will be studied and their subsequent applications in OLEDs will be explored.

5. References:

1. Hong, G. *et al.* A Brief History of OLEDs—Emitter Development and Industry Milestones. *Adv. Mater.* **33**, 2005630 (2021).
2. Koden, M. *OLED Displays and Lighting*. (IEEE Press, Piscataway, 2017).
3. *Organic Optoelectronic Materials*. vol. 91 (Springer International Publishing, Cham, 2015).
4. Tang, C. W., VanSlyke, S. A. & Chen, C. H. Electroluminescence of doped organic thin films. *J. Appl. Phys.* **65**, 3610–3616 (1989).
5. Rothberg, L. J. & Lovinger, A. J. Status of and prospects for organic electroluminescence. *J. Mater. Res.* **11**, 3174–3187 (1996).
6. Dong, X. *et al.* Novel Deuterated Benzothiadiazole Derivatives with Enhancing High-Lying Reverse Intersystem Crossing for High-Efficiency Organic Light-Emitting Diodes. *J. Phys. Chem. C* **128**, 974–983 (2024).
7. Birks, J. B. *Photophysics of Aromatic Molecules*. (Wiley-Interscience, London, New York, 1970).
8. Baldo, M. A. *et al.* Highly efficient phosphorescent emission from organic electroluminescent devices. *Nature* **395**, 151–154 (1998).
9. Zhao, W., He, Z. & Tang, B. Z. Room-temperature phosphorescence from organic aggregates. *Nat. Rev. Mater.* **5**, 869–885 (2020).
10. Chen, C.-H. *et al.* High-Performance Deep-Blue OLEDs Harnessing Triplet–Triplet Annihilation Under Low Dopant Concentration. *Adv. Photonics Res.* **4**, 2200204 (2023).
11. Uoyama, H., Goushi, K., Shizu, K., Nomura, H. & Adachi, C. Highly efficient organic light-emitting diodes from delayed fluorescence. *Nature* **492**, 234–238 (2012).
12. Chen, X.-K., Kim, D. & Brédas, J.-L. Thermally Activated Delayed Fluorescence (TADF) Path toward Efficient Electroluminescence in Purely Organic Materials: Molecular Level Insight. *Acc. Chem. Res.* **51**, 2215–2224 (2018).
13. Gan, Y. *et al.* Multiple charge transfer disk-like emitters with fast fluorescence radiation rate and high horizontal dipole orientation for pure blue organic light-emitting diodes. *Chem. Eng. J.* **430**, 133030 (2022).

14. Hatakeyama, T. *et al.* Ultrapure Blue Thermally Activated Delayed Fluorescence Molecules: Efficient HOMO–LUMO Separation by the Multiple Resonance Effect. *Adv. Mater.* **28**, 2777–2781 (2016).
15. Pershin, A. *et al.* Highly emissive excitons with reduced exchange energy in thermally activated delayed fluorescent molecules. *Nat. Commun.* **10**, 597 (2019).
16. Madayanad Suresh, S., Hall, D., Beljonne, D., Olivier, Y. & Zysman-Colman, E. Multiresonant Thermally Activated Delayed Fluorescence Emitters Based on Heteroatom-Doped Nanographenes: Recent Advances and Prospects for Organic Light-Emitting Diodes. *Adv. Funct. Mater.* **30**, 1908677 (2020).
17. Adachi, C. Third-generation organic electroluminescence materials. *Jpn. J. Appl. Phys.* **53**, 060101 (2014).
18. Devi, H. R., Bisen, O. Y., Nanda, S., Nandan, R. & Nanda, K. K. Internal versus external quantum efficiency of luminescent materials, photovoltaic cells, photodetectors and photoelectrocatalysis. *Curr. Sci.* **121**, 894 (2021).
19. Nakanotani, H. *et al.* High-efficiency organic light-emitting diodes with fluorescent emitters. *Nat. Commun.* **5**, 4016 (2014).
20. Takada, N., Tsutsui, T. & Saito, S. Control of emission characteristics in organic thin-film electroluminescent diodes using an optical-microcavity structure. *Appl. Phys. Lett.* **63**, 2032–2034 (1993).
21. Li, K. *et al.* Highly phosphorescent platinum(II) emitters: photophysics, materials and biological applications. *Chem. Sci.* **7**, 1653–1673 (2016).
22. Wei, Y.-C. & Hsu, L.-Y. Polaritonic Huang–Rhys Factor: Basic Concepts and Quantifying Light–Matter Interactions in Media. *J. Phys. Chem. Lett.* **14**, 2395–2401 (2023).
23. Ansari, R., Shao, W., Yoon, S.-J., Kim, J. & Kieffer, J. Charge Transfer as the Key Parameter Affecting the Color Purity of Thermally Activated Delayed Fluorescence Emitters. *ACS Appl. Mater. Interfaces* **13**, 28529–28537 (2021).
24. Wu, S. *et al.* Excited-State Modulation in Donor-Substituted Multiresonant Thermally Activated Delayed Fluorescence Emitters. *ACS Appl. Mater. Interfaces* **14**, 22341–22352 (2022).
25. Santoro, F., Lami, A., Improta, R., Bloino, J. & Barone, V. Effective method for the computation of optical spectra of large molecules at finite temperature including

the Duschinsky and Herzberg–Teller effect: The Qx band of porphyrin as a case study. *J. Chem. Phys.* **128**, 224311 (2008).

26. Bersuker, I. B. *The Jahn-Teller Effect*. (Cambridge University Press, Cambridge, UK ; New York, 2006).
27. Kondo, Y. *et al.* Narrowband deep-blue organic light-emitting diode featuring an organoboron-based emitter. *Nat. Photonics* **13**, 678–682 (2019).
28. Hirai, H. *et al.* One-Step Borylation of 1,3-Diaryloxybenzenes Towards Efficient Materials for Organic Light-Emitting Diodes. *Angew. Chem. Int. Ed.* **54**, 13581–13585 (2015).
29. Yuan, Y. *et al.* The Design of Fused Amine/Carbonyl System for Efficient Thermally Activated Delayed Fluorescence: Novel Multiple Resonance Core and Electron Acceptor. *Adv. Opt. Mater.* **7**, 1801536 (2019).
30. Hall, D. *et al.* Improving Processability and Efficiency of Resonant TADF Emitters: A Design Strategy. *Adv. Opt. Mater.* **8**, 1901627 (2020).
31. Sun, D. *et al.* The design of an extended multiple resonance TADF emitter based on a polycyclic amine/carbonyl system. *Mater. Chem. Front.* **4**, 2018–2022 (2020).
32. Zou, S.-N. *et al.* Fully Bridged Triphenylamine Derivatives as Color-Tunable Thermally Activated Delayed Fluorescence Emitters. *Org. Lett.* **23**, 958–962 (2021).
33. Becke, A. D. Density-functional exchange-energy approximation with correct asymptotic behavior. *Phys. Rev. A* **38**, 3098–3100 (1988).
34. Lee, C., Yang, W. & Parr, R. G. Development of the Colle-Salvetti correlation-energy formula into a functional of the electron density. *Phys. Rev. B* **37**, 785–789 (1988).
35. Chatterjee, A. *et al.* Engineering TADF, mechanochromism, and second harmonic up-conversion properties in regioisomeric substitution space. *Chem. Sci.* **14**, 13832–13841 (2023).
36. Qiu, X. *et al.* Narrowband Emission from Organic Fluorescent Emitters with Dominant Low-Frequency Vibronic Coupling. *Adv. Opt. Mater.* **9**, 2001845 (2021).
37. Ishiyama, T., Murata, M. & Miyaura, N. Palladium(0)-Catalyzed Cross-Coupling Reaction of Alkoxydiboron with Haloarenes: A Direct Procedure for Arylboronic Esters. *J. Org. Chem.* **60**, 7508–7510 (1995).

38. Ye, X. *et al.* Narrow-Band Orange–Red Emission Organic Luminophore with Dominant Low-Frequency Vibronic Coupling. *Energy Fuels* **35**, 19139–19145 (2021).
39. Ihn, S. *et al.* An Alternative Host Material for Long-Lifespan Blue Organic Light-Emitting Diodes Using Thermally Activated Delayed Fluorescence. *Adv. Sci.* **4**, 1600502 (2017).
40. Chatterjee, A. *et al.* Emergence of Aggregation Induced Emission (AIE), Room-Temperature Phosphorescence (RTP), and Multistimuli Response from a Single Organic Luminogen by Directed Structural Modification. *J. Phys. Chem. B* **125**, 12832–12846 (2021).
41. Song, H. *et al.* Solvent modulated excited state processes of push–pull molecule with hybridized local excitation and intramolecular charge transfer character. *Phys. Chem. Chem. Phys.* **21**, 3894–3902 (2019).
42. Del Valle, J. C. & Catalán, J. Kasha's rule: a reappraisal. *Phys. Chem. Chem. Phys.* **21**, 10061–10069 (2019).

6. Appendix

6.1. HRMS: QAO-1:

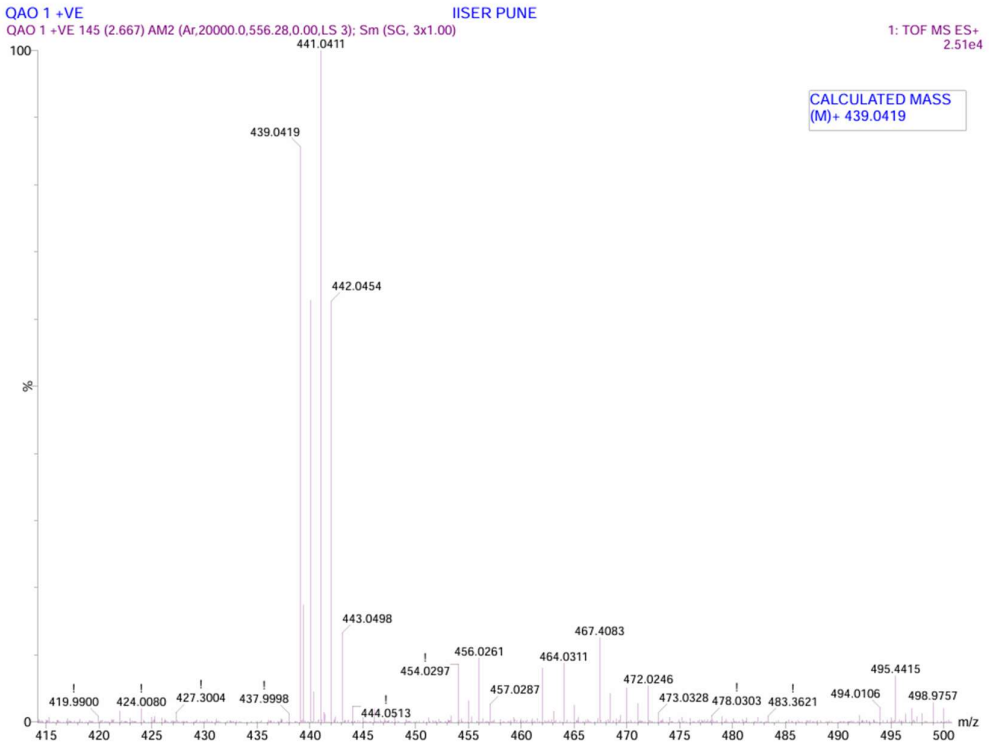

6.2. HRMS: QAO-2:

6.3. HRMS: QAO-Br:

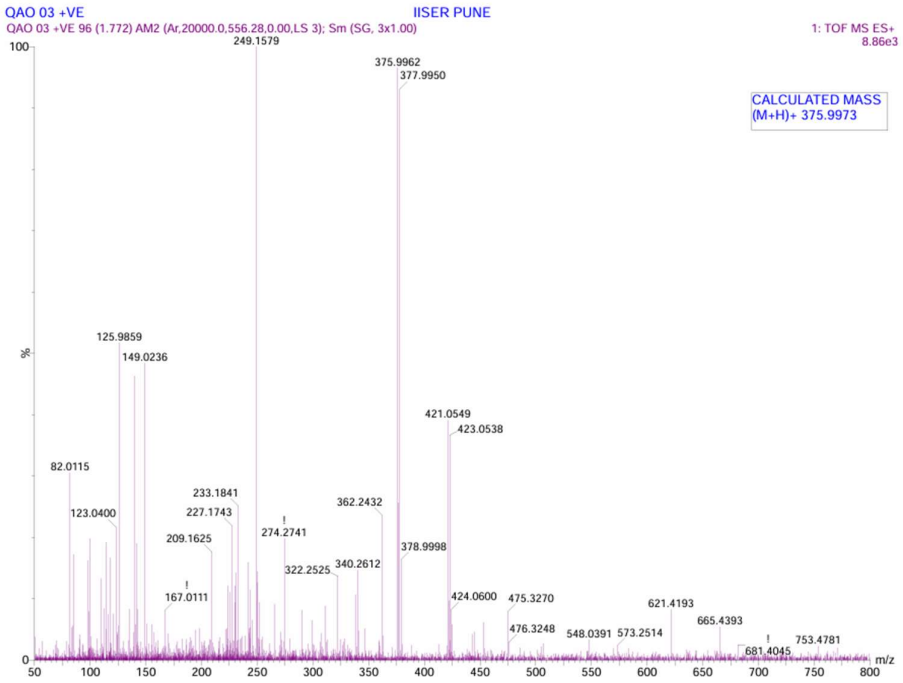

6.4. ^{1}H NMR: QAO-Br:

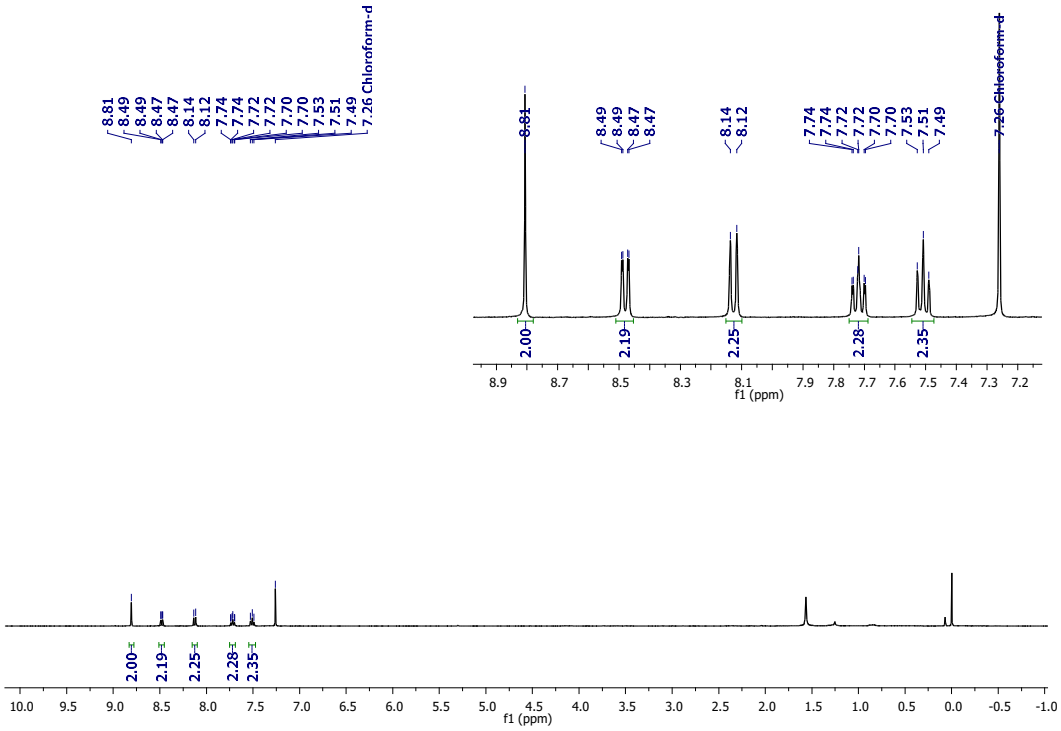

6.5. ^{1}H NMR: CZ-BN-1:

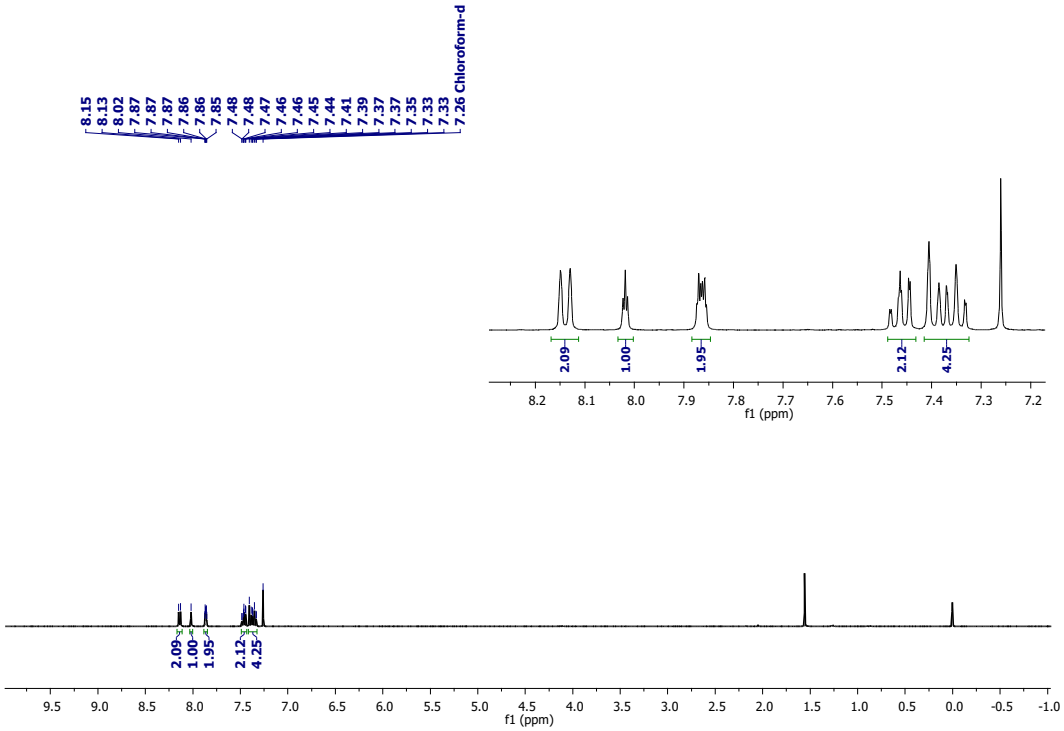

6.6. ^{13}C NMR: CZ-BN-1:

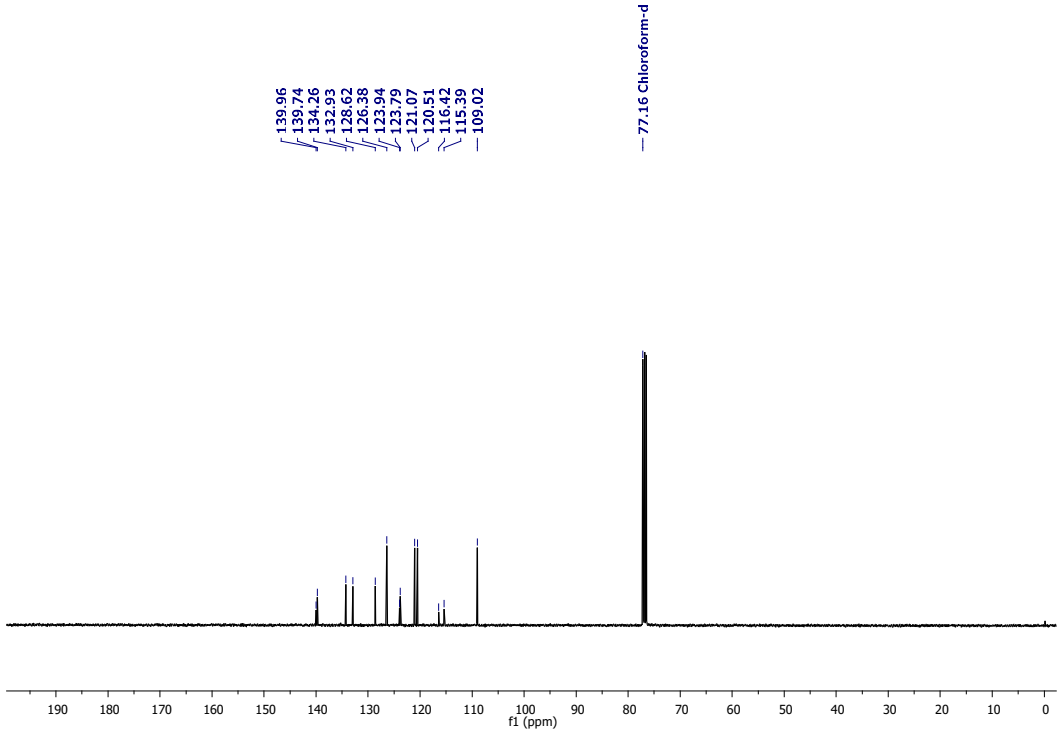

6.7. HRMS: DPA-BN-1:

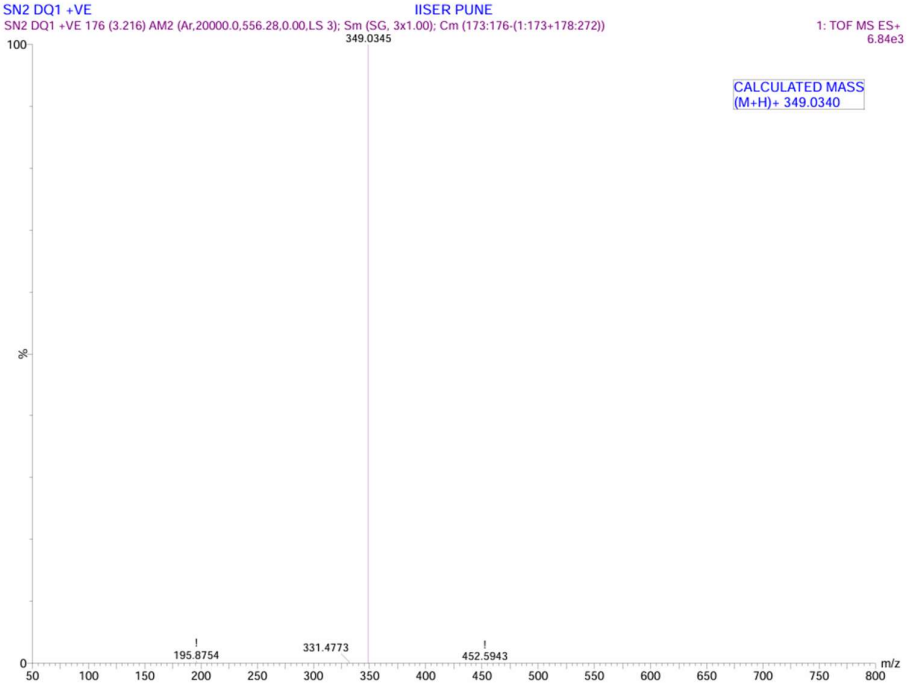

6.8. ^{1}H NMR: DPA-BN-1:

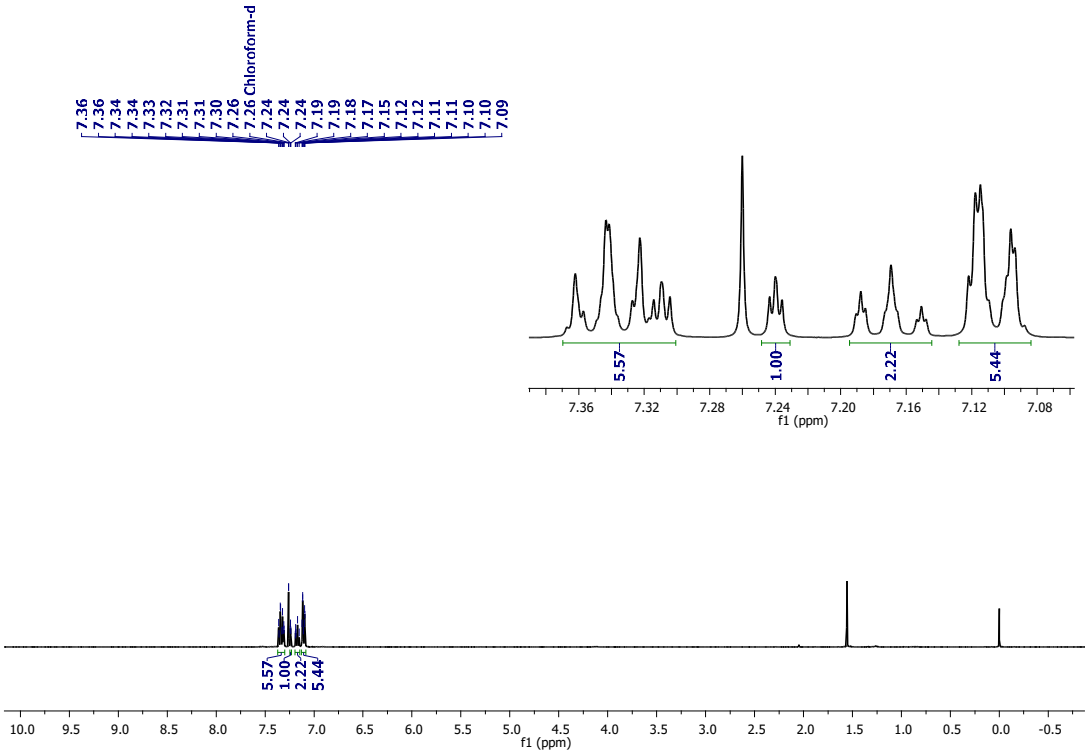

6.9. ^{13}C NMR: DPA-BN-1:

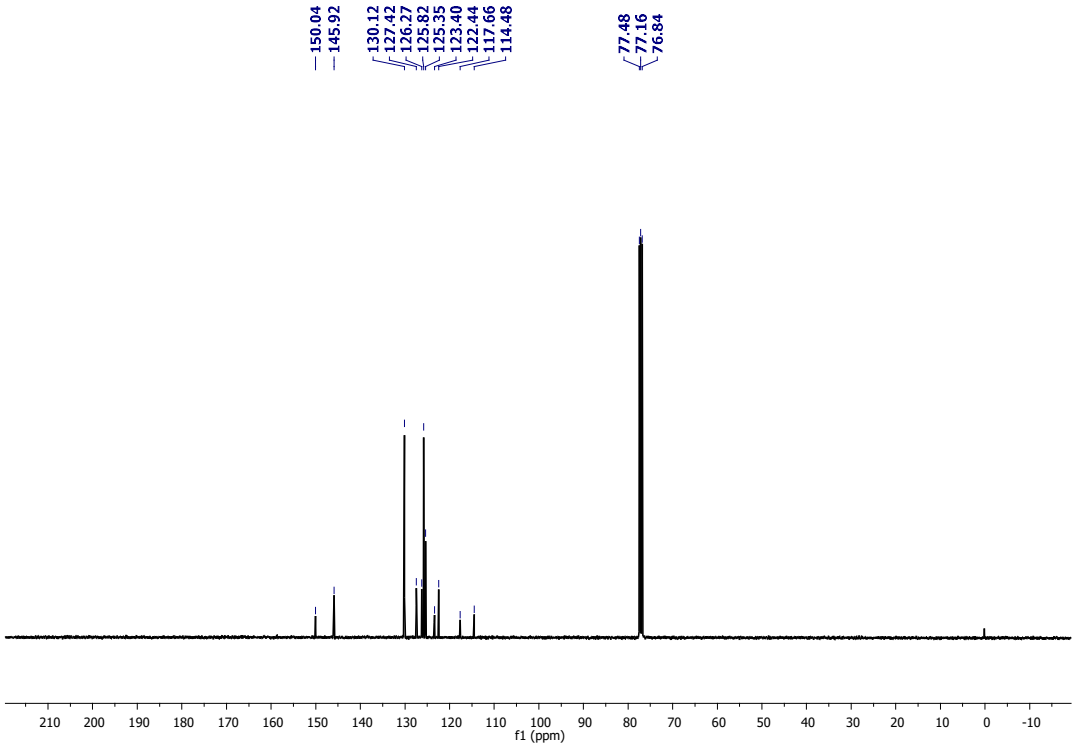

6.10. HRMS: CZ-QAO:

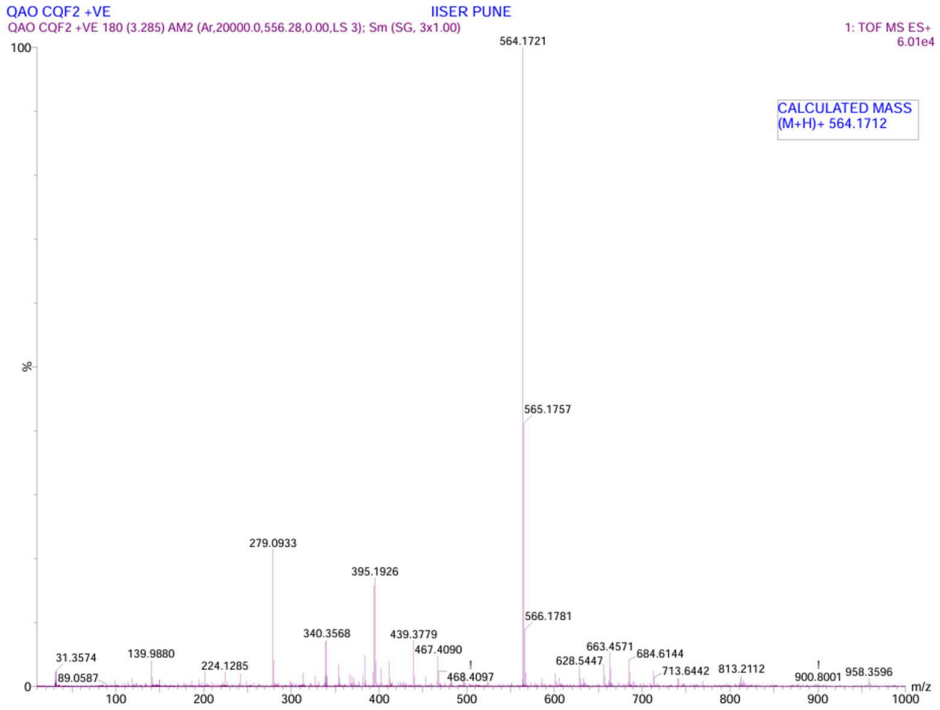

6.11. ^{1}H NMR: CZ-QAO:

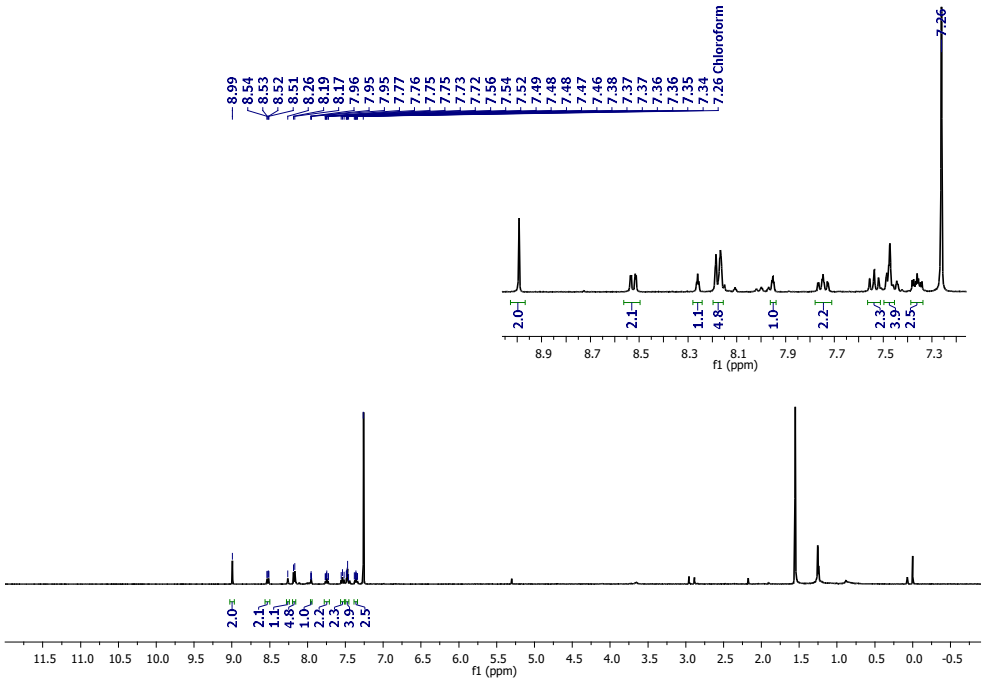

6.12. HRMS: DPA-QAO:

6.13. Quantum Yield calculation of CZQAO in degassed toluene:

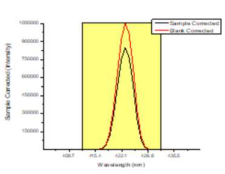

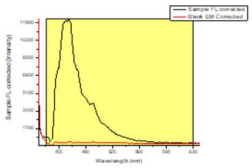

Excitation / Scatter			Emission / Fluorescence		
Enter Start and End Wavelengths			Enter Start and End Wavelengths		
Start Wavelength	412.080	Area Balance Factor	Start Wavelength	438.120	
End Wavelength	432.120	1	End Wavelength	630.000	
Area		Err	Area		Err
La	4.23E+06	2056.89954	*Ea*	518270.32	719.90994
Lc	5.26E+06	2293.19486	*Ec*	54682.28	233.84242

Quantum Yield	45.10
Abs Error±	0.243
Relative Err ±	0.00538

Sample Source CZQAOT4G

HORIBA

Blank Source CZQAOT3G

Calculation

$k_r(S_1–S_0) = \phi_{PF}/\tau_{PF}$

$k_{ISC}(S_1–T_1) = (1–\phi_{PF})/\tau_{PF}$

$k_{RISC}(T_1–S_1) = \phi_{DF}/(k_{ISC}.\tau_{PF}.\tau_{DF}.\phi_{PF})$